Use of MRI in Differentiation of Papillary Renal Cell Carcinoma Subtypes: Qualitative and Quantitative Analysis

Ankur M. Doshi[1]
Justin M. Ream[1]
Andrea S. Kierans[2]
Matthew Bilbily[1]
Henry Rusinek[1]
William C. Huang[3]
Hersh Chandarana[1]

OBJECTIVE. The purpose of this study was to determine whether qualitative and quantitative MRI feature analysis is useful for differentiating type 1 from type 2 papillary renal cell carcinoma (PRCC).

MATERIALS AND METHODS. This retrospective study included 21 type 1 and 17 type 2 PRCCs evaluated with preoperative MRI. Two radiologists independently evaluated various qualitative features, including signal intensity, heterogeneity, and margin. For the quantitative analysis, a radiology fellow and a medical student independently drew 3D volumes of interest over the entire tumor on T2-weighted HASTE images, apparent diffusion coefficient parametric maps, and nephrographic phase contrast-enhanced MR images to derive first-order texture metrics. Qualitative and quantitative features were compared between the groups.

RESULTS. For both readers, qualitative features with greater frequency in type 2 PRCC included heterogeneous enhancement, indistinct margin, and T2 heterogeneity (all, $p < 0.035$). Indistinct margins and heterogeneous enhancement were independent predictors (AUC, 0.822). Quantitative analysis revealed that apparent diffusion coefficient, HASTE, and contrast-enhanced entropy were greater in type 2 PRCC ($p < 0.05$; AUC, 0.682–0.716). A combined quantitative and qualitative model had an AUC of 0.859. Qualitative features within the model had interreader concordance of 84–95%, and the quantitative data had intraclass coefficients of 0.873–0.961.

CONCLUSION. Qualitative and quantitative features can help discriminate between type 1 and type 2 PRCC. Quantitative analysis may capture useful information that complements the qualitative appearance while benefiting from high interobserver agreement.

Keywords: papillary renal cell carcinoma, texture

DOI:10.2214/AJR.15.15004

Received May 7, 2015; accepted after revision October 11, 2015.

Based on a presentation at the Society of Abdominal Radiology 2015 annual meeting, Coronado, CA.

[1]Department of Radiology, Center for Biomedical Imaging, NYU School of Medicine, NYU Langone Medical Center, 660 First Ave, 3rd Fl, New York, NY 10016. Address correspondence to A. M. Doshi (ankur.doshi@nyumc.org).

[2]Department of Radiology, New York-Presbyterian Hospital–Weill Cornell Medical Center, New York, NY.

[3]Department of Urology, Division of Urologic Oncology, NYU Langone Medical Center, New York, NY.

AJR 2016; 206:566–572

0361–803X/16/2063–566

Papillary renal cell carcinoma (PRCC) comprises 10–15% of all renal cell carcinomas, making it the second most common subtype after clear cell RCC [1]. Previous studies have shown that PRCC has more favorable outcomes than clear cell RCC, including a lower incidence of metastasis and a better survival rate [1, 2]. However, despite the overall better prognosis of PRCC, discrete type 1 and type 2 histologic subtypes of PRCC have been identified, and each has distinct biologic behavior [3]. Several series have shown that type 2 PRCC is associated with higher nuclear grade, higher pathologic stage, and poorer survival than type 1 PRCC [2, 4–7]. Because of the aggressiveness of type 2 tumors, conservative treatment options, such as surveillance, percutaneous ablation, and nephron-sparing procedures, may not be appropriate. Furthermore, adjuvant treatment and modified postsurgical surveillance protocols may be warranted for high-risk tumor subtypes [2, 8].

MRI has excellent utility in differentiating PRCC from other renal neoplasms on the basis of T2 signal intensity, apparent diffusion coefficient (ADC) map values, and enhancement pattern [9, 10]. Because evolving strategies for management of small incidental renal masses include less aggressive percutaneous ablation and even active surveillance, prediction of type 2 PRCC through imaging is important for appropriate therapy, given the aggressive behavior of the tumors. Previous studies have not shown imaging features on conventional MR images that are reliable for differentiating PRCC subtypes [11, 12]. Although type 2 PRCC has been found to have indistinct margins on CT images and heterogeneous signal intensity on MR images, the overlap with type 1 tumors limits the utility of these qualitative features for prospective differentiation of PRCC subtype [11, 13].

Quantitative texture analysis has emerged as a valuable tool for the evaluation of various malignancies and has shown promise for

TABLE 1: Demographics of 37 Patients With 38 Papillary Renal Cell Carcinomas

Characteristic	Type of Papillary Renal Cell Carcinoma	
	1	2
Sex[a]		
Male	20 (88.2)	14 (87.5)
Female	1 (11.8)	2 (12.5)
Age[b]	57.5 (36–80)	63.2 (41–81)
Size (cm)[c]	2.9 ± 1.9 (0.9–8)	4.7 ± 3.5 (1.2–15.5)
Side[a]		
Left	12 (57.1)	9 (52.9)
Right	9 (42.9)	8 (47.1)
Pathologic stage[a]		
1	19 (90.5)	13 (76.5)
2	2 (9.5)	2 (11.8)
3	0 (0)	2 (11.8)
4	0 (0)	0 (0)

[a]Data are raw number with percentage in parentheses. Type 2 percentages do not always total 100 owing to rounding.
[b]Data are mean with range in parentheses.
[c]Data are mean ± SD with range in parentheses.

differentiation and outcome prediction of renal masses [14, 15]. This technique extracts pixel intensity and position data that may not be visible to the naked eye, thus it may afford more accurate and reliable lesion characterization. First-order texture metrics are derived from analysis of pixel intensity histograms and include measures such as mean intensity, kurtosis (histogram flatness), entropy (irregularity), and skewness (histogram asymmetry) [15]. Although several studies have shown encouraging results deriving texture parameters from a single 2D slice, results of whole-tumor analysis encompassing the entire 3D tumor volume have been found to be more representative of heterogeneity [16–19].

The purpose of our study was to evaluate the performance of quantitative whole-tumor volume histogram analysis and qualitative feature assessment for the differentiation of type 1 from type 2 PRCC on MRI. We hypothesized that quantitative analysis would have complementary diagnostic utility.

Materials and Methods

Subjects

This retrospective study was approved by the institutional review board with waiver of informed consent and was HIPAA compliant. We searched our nephrectomy database for patients with PRCC who had undergone preoperative MRI, and we identified 59 tumors. Tumors were excluded for the following reasons: pathology report not specifying PRCC subtype (n = 17), lack of diagnostic-quality DWI in preoperative MRI (n = 3), and size smaller than 1 cm (n = 1). The final cohort was 38 PRCCs (type 1, 21; type 2, 17) in 37 patients. One patient had two tumors, both type 2 PRCC. Patient demographic information and tumor characteristics are shown in Table 1.

MRI Technique

MRI examinations were performed with 1.5-T systems (Magnetom Sonata, Symphony, or Avanto, Siemens Healthcare). Because multiple MRI units were used and the technologist adjusted acquisition parameters to optimize the study, representative sequence parameters are provided. These included the following: axial 2D T1-weighted in- and opposed-phase gradient-echo sequences (TR, 160–200 ms; opposed-phase TE, 2.0–2.5 ms; in-phase TE, 4.2–5.0 ms; flip angle, 80°; 70–80% rectangular FOV, 300–500 mm^2; matrix, 112–208 × 256; section thickness, 6–8 mm); axial or coronal HASTE (TR/TE, infinite/62–103; flip angle, 150–180°; FOV, 325–500 mm^2; matrix, 179–320 × 256–380; section thickness, 4–6 mm); and axial fat-suppressed single-shot echo-planar DWI with b values of 0, 400, and 800 s/mm^2 (TR/TE, 1500–2000/65–86; 70–80% rectangular FOV, 325–500 mm^2; matrix, 144–192 × 192; section thickness, 6–8 mm). ADC maps were constructed at the MRI unit by means of monoexponential fit. Axial unenhanced and gadolinium-enhanced 3D fat-suppressed spoiled gradient-echo T1-weighted volume interpolated breath-hold acquisitions were also performed (TR/TE, 3.1–4.5/1.1–1.9; flip angle, 12°; 70–80% rectangular FOV, 300–500-mm; matrix, 125–175 × 256; section thickness, 2–3 mm). The contrast-enhanced images were acquired during the corticomedullary, nephrographic, and excretory phases after administration of 0.1 mmol/kg gadopentetate dimeglumine (Magnevist, Bayer HealthCare), which was injected at 2 mL/s and followed by a 20-mL saline bolus.

Qualitative MRI Analysis

For the qualitative analysis, two blinded radiologists (readers 1 and 2) with fellowship training in abdominal imaging and 1 year of experience independently evaluated the images. The following tumor features were assessed: tumor size, visible loss of signal intensity on T1-weighted in-phase images (indicating hemosiderin), T1 and T2 signal intensity, heterogeneity in relation to renal cortex, DWI signal intensity in relation to cortex (highest b value), margin distinctness on contrast-enhanced images, enhancement heterogeneity in the nephrographic phase, hypovascularity (tumor signal intensity less than renal cortex signal intensity on nephrographic phase contrast-enhanced images), and necrosis on HASTE and contrast-enhanced images.

In a subsequent qualitative analysis, the abdominal radiologist (reader 2) and an abdominal imaging fellow (reader 4) independently reviewed each patient's complete MRI examination and provided an overall diagnostic impression of either type 1 or type 2 PRCC based only on qualitative features. For this analysis, sensitivity and specificity and interreader concordance were computed.

Quantitative MRI Analysis

For the quantitative analysis, locally developed software (Firevoxel) was used to draw 3D volumes of interest (VOIs) over the entire tumor on the ADC maps and HASTE and nephrographic phase contrast-enhanced images. This task was performed independently by two readers, a medical student (reader 3) and the abdominal imaging fellow (reader 4). Both readers underwent a training session and were given detailed instructions on how to use the software to draw the largest VOI possible over every slice that contained the tumor while avoiding the extreme edge. The VOI file and histogram information were saved to a file and processed separately. For ADC, HASTE, and contrast-enhanced images, skewness, kurtosis, and entropy were computed. For ADC, mean signal intensity was also computed.

Statistical Analysis

For the qualitative analysis, standard summary statistics were used to calculate frequencies of imaging features seen in each PRCC subtype. A Fisher exact test and binary logistic regression were

TABLE 2: Qualitative MRI Feature Analysis of Papillary Renal Cell Carcinoma (PRCC)

Feature	Reader 1			Reader 2			Interreader Concordance (%)
	Type 1 PRCC	Type 2 PRCC	p[a]	Type 1 PRCC	Type 2 PRCC	p[a]	
No. of tumors	21	17		21	17		
Hemosiderin present	2 (9.5)	3 (17.6)	0.640	8 (38.1)	8 (47.1)	0.743	71
T2 hypointense	15 (71.4)	8 (47.1)	0.185	15 (71.4)	8 (47.1)	0.185	79
T2 heterogeneous	11 (52.4)	15 (88.2)	**0.034**	11 (52.4)	16 (94.1)	**0.010**	92
Hyperintense DWI	20 (95.2)	15 (88.2)	0.577	21 (100)	16 (94.1)	0.447	89
T1 isointense or hyperintense	19 (90.5)	16 (94.1)	1	17 (81.0)	15 (88.2)	0.672	82
T1 heterogeneous	15 (71.4)	13 (76.5)	1	9 (42.9)	14 (82.4)	**0.025**	74
Indistinct tumor margin	1 (4.8)	8 (47.1)	**0.005**	0 (0)	9 (52.9)	**0.0001**	84
Hypovascular	19 (90.5)	14 (82.4)	0.640	20 (95.2)	17 (100)	1	89
Heterogeneous enhancement	10 (47.6)	16 (94.1)	**0.004**	11 (52.4)	15 (88.2)	**0.034**	95
Necrosis	1 (4.8)	2 (11.8)	0.577	2 (9.5)	4 (23.5)	0.378	87

Note—Except for number of tumors, data are raw number with percentage in parentheses.
[a]Fisher exact test. **Bold type** indicates $p < 0.05$.

used to assess for associations between qualitative imaging features and papillary subtype. For the quantitative analysis, a Mann-Whitney exact test was used to compare mean histogram measures between papillary subtypes. Stepwise variable selection in the context of binary logistic regression was used to identify combinations of quantitative and qualitative imaging features representing significant independent predictors of papillary subtype. In the search for only independent predictors of a given type (either quantitative or qualitative), the results from the two readers providing the respective measure were combined into a single overall dataset. Because the readers providing qualitative data (readers 1 and 2) were different from those providing quantitative data (readers 3 and 4), the analysis to examine combinations of both binary and numeric measures predictive of papillary subtype was based on a combined dataset consisting of results from all four combinations of the two groups of readers. In particular, in the combined dataset, the data for each subject consisted of numeric measures from reader 1 combined with binary measures from reader 3 and of corresponding sets of results for reader pairs 1 and 4, 2 and 3, and 2 and 4. Interreader concordance for qualitative analysis was determined by calculating the frequency with which both readers rendered the same assessment for each imaging feature. For the quantitative analysis, interreader agreement was measured using intraclass correlation (< 0.2 indicating no agreement; 0.21–0.40, poor agreement; 0.41–0.60, fair to moderate agreement; 0.61–0.80, good to substantial agreement; > 0.81, very good to excellent agreement). All statistical tests were conducted at the two-sided 5% significance level with SAS software (version 9.3, SAS Institute).

Results

The results of the qualitative MRI feature analysis are presented in Table 2. Features present significantly more frequently in type

TABLE 3: Quantitative First-Order Texture Parameters of Type 1 and Type 2 Papillary Renal Cell Carcinomas (PRCCs)

Value	Reader 3			Reader 4		
	Type 1 PRCC	Type 2 PRCC	p[a]	Type 1 PRCC	Type 2 PRCC	p[a]
Apparent diffusion coefficient						
Mean	105.55 ± 35.87	122.72 ± 44.00	0.102	112.76 ± 38.26	119.71 ± 42.57	0.302
Skewness	0.15 ± 0.51	0.19 ± 0.42	0.883	0.11 ± 0.60	0.20 ± 0.39	0.930
Kurtosis	0.12 ± 0.89	0.18 ± 0.76	0.618	0.35 ± 0.80	0.20 ± 0.77	0.618
Entropy	4.29 ± 0.59	4.71 ± 0.44	**0.026**	4.40 ± 0.48	4.70 ± 0.46	**0.049**
Contrast-enhanced						
Skewness	0.19 ± 0.39	0.52 ± 1.14	0.481	0.38 ± 0.30	0.41 ± 0.78	0.883
Kurtosis	0.24 ± 0.74	0.47 ± 1.03	0.792	0.42 ± 1.13	0.46 ± 0.89	0.445
Entropy	4.14 ± 0.67	4.65 ± 0.49	**0.026**	4.27 ± 0.62	4.72 ± 0.42	**0.026**
HASTE						
Skewness	0.49 ± 0.66	0.48 ± 0.54	0.649	0.52 ± 0.62	0.53 ± 0.54	0.639
Kurtosis	0.60 ± 1.89	0.41 ± 0.93	0.670	0.67 ± 1.90	0.66 ± 1.19	0.577
Entropy	4.71 ± 0.75	5.27 ± 0.57	0.058	4.85 ± 0.63	5.34 ± 0.50	**0.035**

Note—Data are mean ± SD.
[a]Mann-Whitney test. **Bold type** indicates $p < 0.05$.

2 than type 1 PRCC for both readers 1 and 2 included T2 heterogeneity (reader 1, 88.2% vs 52.4%; reader 2, 94.1% vs 52.4%), indistinct tumor margin (reader 1, 47.1% vs 4.8%; reader 2, 52.9% vs 0%), and heterogeneous enhancement in the nephrographic phase (reader 1, 94.1% vs 47.6%; reader 2, 88.2% vs 52.4%) (all, $p < 0.035$). Examples of lesions are shown in Figures 1 and 2. T1 heterogeneity was statistically significant only for reader 2 (Table 2).

The presence of hemosiderin, T2 signal intensity, diffusion signal intensity, T1 hyperintensity, T1 heterogeneity, enhancement in relation to renal cortex, and necrosis did not show a statistical difference between the PRCC subtypes (Table 2). Interreader concordance ranged from 71% to 95%. Multivariate logistic regression analysis revealed that indistinct margin ($p = 0.004$) and heterogeneous enhancement ($p = 0.019$) were independent predictors of papillary subtype, together having an AUC of 0.822.

The separate qualitative analysis in which two readers (readers 2 and 4) independently used all available MRI sequences to predict PRCC subtype showed sensitivity of 70.6% and 47.1%, specificity of 85.7% and 85.7%, and AUC of 0.78 and 0.66. The interreader concordance for this analysis was 74%.

The quantitative univariate texture analysis revealed that mean entropy was greater in type 2 PRCC than in type 1 PRCC on ADC and contrast-enhanced nephrographic phase images for both readers ($p < 0.05$) (Table 3). HASTE entropy was significantly greater for reader 4 ($p = 0.035$) and nearly reached significance for reader 3 ($p = 0.058$). Skewness, kurtosis, and mean ADC did not have statistically significant differences for either reader. Logistic regression analysis revealed that for reader 3, ADC, nephrographic contrast-enhanced, and HASTE entropy were significant predictors of PRCC subtype (AUC, 0.682–0.716). For reader 4, nephrographic contrast-enhanced and HASTE entropy were predictors of PRCC subtype (AUC, 0.704–0.714). Interreader agreement for entropy was very good to excellent for all sequences, with an intraclass coefficient of 0.899 for ADC, 0.961 for HASTE, and 0.873 for nephrographic phase imaging (Table 4).

When both quantitative and qualitative measures were allowed to compete for inclusion in the prediction model, HASTE entropy ($p = 0.004$), indistinct margin ($p < 0.001$), and heterogeneous enhancement ($p = 0.002$) were identified as independent predictors of papillary subtype, together having an AUC of 0.859. Nearly all (19/21) of the type 1 PRCCs were pathologic stage I; the other two were stage II. Two of 17 type 2 PRCC were stage III, two were stage II, and 13 were stage I.

TABLE 4: Interreader Agreement for Quantitative Analysis Performed With Intraclass Correlation

Value	Intraclass Correlation Coefficient	95% Confidence Limits	
		Low	High
ADC			
Mean	0.799	0.647	0.890
Skewness	0.492	0.204	0.700
Kurtosis	0.473	0.187	0.685
Entropy	0.899	0.814	0.946
HASTE			
Skewness	0.921	0.855	0.958
Kurtosis	0.941	0.887	0.969
Entropy	0.961	0.860	0.984
Contrast-enhanced			
Skewness	0.754	0.576	0.864
Kurtosis	0.713	0.514	0.840
Entropy	0.873	0.763	0.933

Note—ADC = apparent diffusion coefficient.

Discussion

In this study, we identified qualitative MRI features and quantitative first-order textural histogram metrics that are associated with PRCC subtype. For both readers, the presence of indistinct margins and heterogeneous enhancement had good performance for the prediction of PRCC subtype (AUC, 0.822). The quantitative model revealed that entropy measures on nephrographic contrast-enhanced and HASTE images were predictors of PRCC subtype for both readers (AUC, 0.682–0.716). A model combining quantitative and qualitative features revealed that HASTE entropy, indistinct margins, and heterogeneous enhancement were predictors of a subtype with good performance (AUC, 0.859).

Previous studies have shown that type 2 PRCC has indistinct margins on CT images [11, 13], but there was overlap with type 1 tumors. For example, Egbert et al. [11] found that indistinct margins were present in 6% of type 1 and 33% of type 2 PRCCs, whereas Yamada et al. [13] found that 37.5% of type 2 tumors had distinct margins. In our study, indistinct margins were infrequently seen in type 1 PRCC but were seen in approximately one-half of type 2 PRCCs. Our qualitative model showed that tumor margin indistinctness on MR images was an independent predictor, whereas other previous studies did not show such an association [11, 12]. The reason for this difference is unclear, but possible explanations include the smaller number (six) of type 2 PRCCs in one study [11] or the poorer spatial resolution of MRI compared with CT, which may make it more difficult to detect subtle areas of margin indistinctness. In our study, both readers were instructed to assess tumor margin on the contrast-enhanced images, which have 2-mm slice thickness (interpolated) at our institution.

As we did, other investigators found overlap in tumor heterogeneity on both CT and MR images. Although Egbert et al. [11] found that all type 2 PRCCs were heterogeneous in at least one MRI sequence, nearly one-half of type 1 tumors also exhibited this feature. In our study, we also found overlap of these imaging features: approximately one-half of type 1 PRCCs were heterogeneous on T2-weighted and contrast-enhanced images.

Subjective qualitative assessment is prone to interreader variability, as observed in our study, in which interreader concordance was as low as 71% for certain features. The interreader concordance for overall prediction of subtype when only qualitative features were used was 74%. These factors somewhat limit the role of qualitative feature assessment alone in guiding clinical management and warrant evaluation of other potential diagnostic criteria, such as quantitative factors.

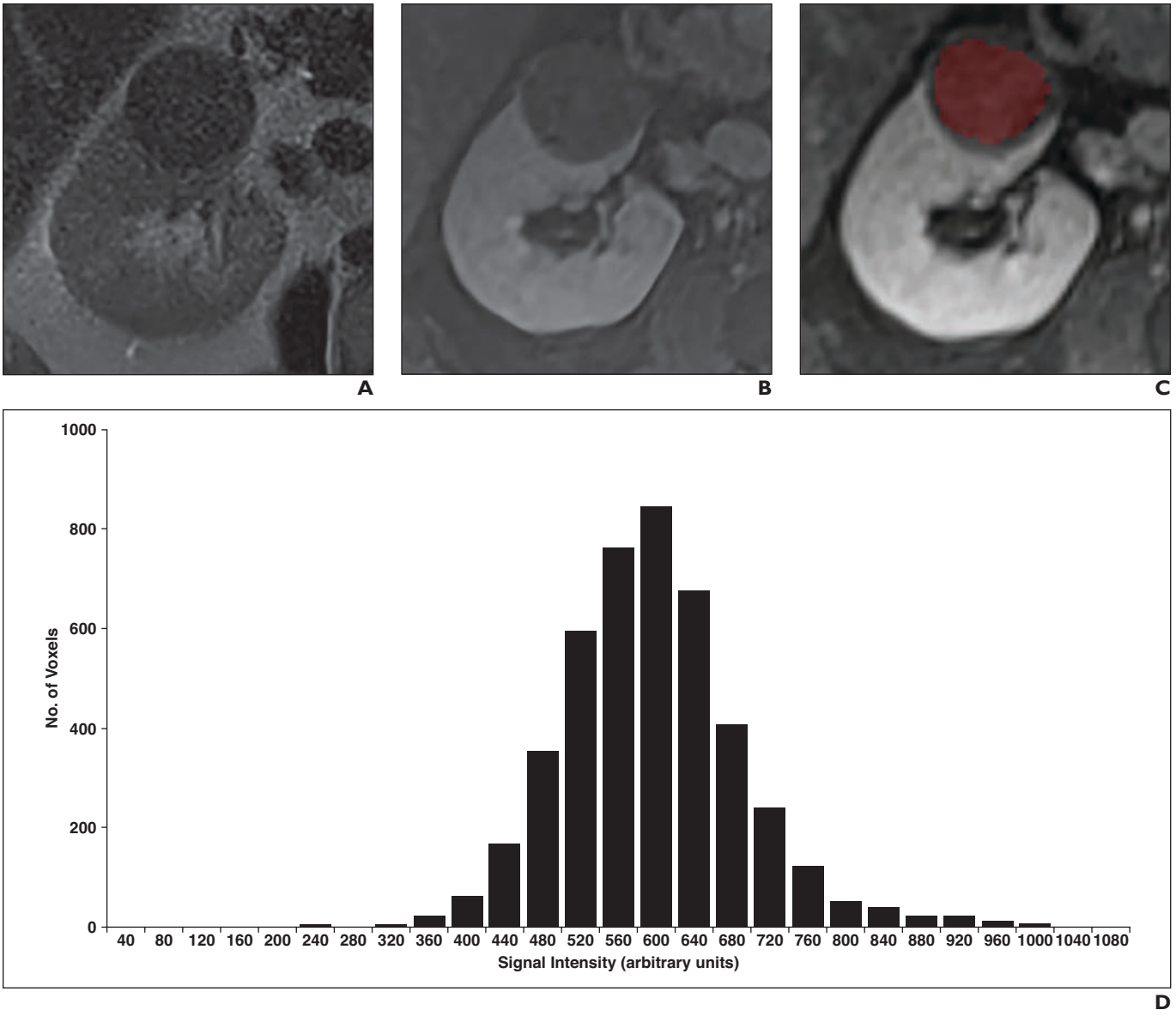

Fig. 1—43-year-old man with 4.2-cm type 1 papillary renal cell carcinoma.
A, Axial HASTE MR image shows homogeneous T2 hypointensity.
B, Axial T1-weighted contrast-enhanced MR image shows homogeneous enhancement with well-defined margin.
C, Contrast-enhanced MR image shows shaded volume of interest drawn over whole lesion.
D, Corresponding histogram of signal intensities binned by factor of 40 reveals mean entropy of 3.62 for both readers.

Quantitative analysis has several advantages, including minimization of variability related to reader subjectivity, as found in our study, in which there was very good to excellent interreader agreement. Although our quantitative model alone had worse AUCs than the qualitative model for subtype prediction, the combined model had slightly better AUCs. A possible cause of the poorer performance of the quantitative model is that the readers were instructed to draw the largest VOI possible over the tumor while avoiding the extreme edge. This was done to avoid the effects of volume averaging with the adjacent renal parenchyma or fat, but the consequence of such a technique is that data regarding tumor margin are lost. Because the qualitative model revealed that margin distinctness was a predictor of tumor subtype, it is possible that use of a more robust quantitative model that extracted information related to lesion margin would have improved performance.

Further refinement of lesion segmentation technique and quantitative modeling may prove to be a useful complementary analytic tool, especially because subjective qualitative feature analyses are prone to interobserver variability and tumor subtype overlap. A model that allows successful prediction of PRCC subtype can help steer patients to appropriate therapy. This therapy may include more timely intervention for aggressive tumors and conservative therapy for indolent lesions, especially in patients whose condition precludes surgery. Furthermore, patients with the more aggressive type 2 PRCC subtype may need a more aggressive postsurgical surveillance protocol.

Research findings have shown the value of texture analysis in various renal applications,

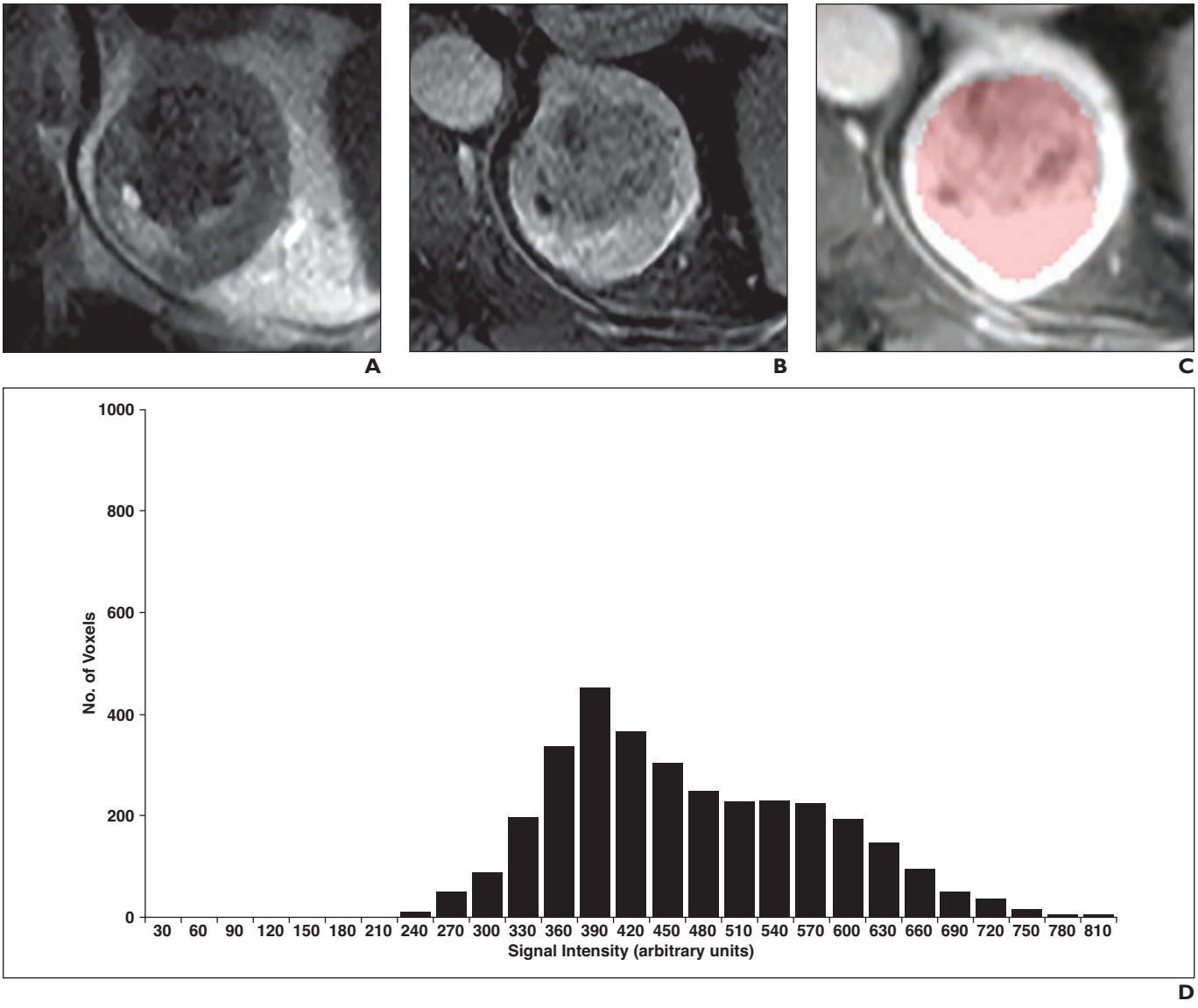

Fig. 2—61-year-old man with 4.8-cm type 2 papillary renal cell carcinoma.
A, Axial HASTE MR image shows heterogeneous T2 signal intensity.
B, Contrast-enhanced T1-weighted MR image shows heterogeneous enhancement with indistinct margins.
C, Contrast-enhanced MR image shows shaded volume of interest drawn over whole lesion.
D, Corresponding histogram of signal intensities binned by factor of 30 reveals mean entropy of 5.82 for both readers.

including tumor classification and prediction of tumor stage and response to chemotherapy [14, 20, 21]. Statistical analysis of histogram variability can be a useful measure of lesion characterization. Kurtosis provides information about the distribution of intensities near the mean; positive kurtosis indicates a greater chance of finding intensity values near the mean, and negative kurtosis indicates a greater chance of encountering extreme values within the tails. Skewness reflects the asymmetry of the histogram; a positive skew indicates a larger tail on the right, and a negative skew indicates a larger tail on the left. Entropy is a measure of the irregularity of gray-level distribution; greater values reflect increased lesion heterogeneity. A random distribution has high entropy, which generally indicates greater heterogeneity [22]. At histologic examination, type 2 PRCC has larger cells with a higher nuclear grade than does type 1 PRCC [3]. It may be possible that the imaging heterogeneity reflects the microscopic structure of type 2 PRCC. ADC entropy has also been found to be useful for lesion evaluation in the adnexa, where investigators found that greater entropy was associated with malignancy [23].

Although texture analysis is a tool that does not require acquisition of additional images during the examination, lesion segmentation and quantitative analysis do require additional time at the point of interpretation. We used locally developed texture analysis software, but there are commercially available (TexRAD, TexRAD, Ltd.) and free (MaZda, Technical University of Lodz) programs. Because these stand-alone software programs allow the import of DICOM image data, PACS compatibility issues are not a major concern.

Several limitations to this study warrant mention. First, it was a retrospective analysis

with a small sample size. We evaluated first-order texture features, which do not reflect spatial information. Drawing of VOIs was done manually, possibly introducing variability, but there was very good to excellent interreader reproducibility. There remains debate as to whether subtyping of PRCC has prognostic significance because not all studies have consistently shown worse outcomes in type 2 PRCC [24]. It has also been acknowledged [24] that correct histologic subtyping requires experience, because other renal tumors can be misclassified as type 2 PRCC. We did not have pathologists rereview the slides for this study because the initial interpretation was performed by pathologists with genitourinary expertise.

Conclusion

Our results show that there are individual qualitative and quantitative features associated with PRCC subtype, but a model combining the two may be a complementary approach that mitigates the limitations of each. Quantitative analysis may capture useful supplementary diagnostic information with the benefit of high interobserver agreement.

References

1. Campbell N, Rosenkrantz AB, Pedrosa I. MRI phenotype in renal cancer: is it clinically relevant? *Top Magn Reson Imaging* 2014; 23:95–115
2. Pignot G, Elie C, Conquy S, et al. Survival analysis of 130 patients with papillary renal cell carcinoma: prognostic utility of type 1 and type 2 subclassification. *Urology* 2007; 69:230–235
3. Delahunt B, Eble JN. Papillary renal cell carcinoma: a clinicopathologic and immunohistochemical study of 105 tumors. *Mod Pathol* 1997; 10:537–544
4. Mejean A, Hopirtean V, Bazin JP, et al. Prognostic factors for the survival of patients with papillary renal cell carcinoma: meaning of histological typing and multifocality. *J Urol* 2003; 170:764–767
5. Waldert M, Haitel A, Marberger M, et al. Comparison of type I and II papillary renal cell carcinoma (RCC) and clear cell RCC. *BJU Int* 2008; 102:1381–1384
6. Klatte T, Pantuck AJ, Said JW, et al. Cytogenetic and molecular tumor profiling for type 1 and type 2 papillary renal cell carcinoma. *Clin Cancer Res* 2009; 15:1162–1169
7. Delahunt B, Eble JN, McCredie MR, Bethwaite PB, Stewart JH, Bilous AM. Morphologic typing of papillary renal cell carcinoma: comparison of growth kinetics and patient survival in 66 cases. *Hum Pathol* 2001; 32:590–595
8. Siddiqui SA, Frank I, Cheville JC, Lohse CM, Leibovich BC, Blute ML. Postoperative surveillance for renal cell carcinoma: a multifactorial histological subtype specific protocol. *BJU Int* 2009; 104:778–785
9. Pedrosa I, Chou MT, Ngo L, et al. MR classification of renal masses with pathologic correlation. *Eur Radiol* 2008; 18:365–375
10. Cornelis F, Tricaud E, Lasserre AS, et al. Routinely performed multiparametric magnetic resonance imaging helps to differentiate common subtypes of renal tumours. *Eur Radiol* 2014; 24:1068–1080
11. Egbert ND, Caoili EM, Cohan RH, et al. Differentiation of papillary renal cell carcinoma subtypes on CT and MRI. *AJR* 2013; 201:347–355
12. Rosenkrantz AB, Sekhar A, Genega EM, et al. Prognostic implications of the magnetic resonance imaging appearance in papillary renal cell carcinoma. *Eur Radiol* 2013; 23:579–587
13. Yamada T, Endo M, Tsuboi M, et al. Differentiation of pathologic subtypes of papillary renal cell carcinoma on CT. *AJR* 2008; 191:1559–1563
14. Raman SP, Chen Y, Schroeder JL, Huang P, Fishman EK. CT texture analysis of renal masses: pilot study using random forest classification for prediction of pathology. *Acad Radiol* 2014; 21:1587–1596
15. Davnall F, Yip CS, Ljungqvist G, et al. Assessment of tumor heterogeneity: an emerging imaging tool for clinical practice? *Insights Imaging* 2012; 3:573–589
16. Miles KA, Ganeshan B, Griffiths MR, Young RC, Chatwin CR. Colorectal cancer: texture analysis of portal phase hepatic CT images as a potential marker of survival. *Radiology* 2009; 250:444–452
17. Ganeshan B, Skogen K, Pressney I, Coutroubis D, Miles K. Tumour heterogeneity in oesophageal cancer assessed by CT texture analysis: preliminary evidence of an association with tumour metabolism, stage, and survival. *Clin Radiol* 2012; 67:157–164
18. Ganeshan B, Panayiotou E, Burnand K, Dizdarevic S, Miles K. Tumour heterogeneity in non-small cell lung carcinoma assessed by CT texture analysis: a potential marker of survival. *Eur Radiol* 2012; 22:796–802
19. Ng F, Kozarski R, Ganeshan B, Goh V. Assessment of tumor heterogeneity by CT texture analysis: can the largest cross-sectional area be used as an alternative to whole tumor analysis? *Eur J Radiol* 2013; 82:342–348
20. Kierans AS, Rusinek H, Lee A, et al. Textural differences in apparent diffusion coefficient between low- and high-stage clear cell renal cell carcinoma. *AJR* 2014; 203:[web]W637–W644
21. Goh V, Ganeshan B, Nathan P, Juttla JK, Vinayan A, Miles KA. Assessment of response to tyrosine kinase inhibitors in metastatic renal cell cancer: CT texture as a predictive biomarker. *Radiology* 2011; 261:165–171
22. Ng F, Ganeshan B, Kozarski R, Miles KA, Goh V. Assessment of primary colorectal cancer heterogeneity by using whole-tumor texture analysis: contrast-enhanced CT texture as a biomarker of 5-year survival. *Radiology* 2013; 266:177–184
23. Kierans AS, Bennett GL, Mussi TC, et al. Characterization of malignancy of adnexal lesions using ADC entropy: comparison with mean ADC and qualitative DWI assessment. *J Magn Reson Imaging* 2013; 37:164–171
24. Delahunt B, Cheville JC, Martignoni G, et al. The International Society of Urological Pathology (ISUP) grading system for renal cell carcinoma and other prognostic parameters. *Am J Surg Pathol* 2013; 37:1490–1504